Solid solution-type Sm-Pr-O supported nickel-based catalysts for auto-thermal reforming of acetic acid: Role of Pr in solid solution

Jinbo Liu[1,2], Jia Huang[2], Chenyu Ding[2], Fuxia Liao[2], Chenghong Shu[2], Lihong Huang[1,2,*]

Author affiliations

[1] State Key Laboratory of Geohazard Prevention and Geoenvironment Protection, Chengdu University of Technology, Chengdu; 610059, China

[2] College of Materials and Chemistry & Chemical Engineering, Chengdu University of Technology, Chengdu 610059, China

[*]Address all correspondence to this author. e-mail: huanglihong06@cdut.cn (L. Huang)

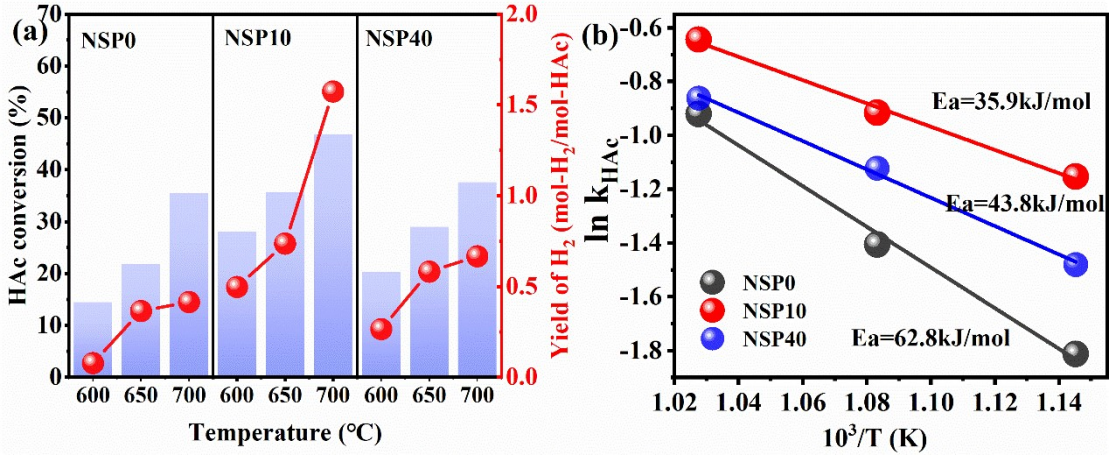

Fig. S1. HAc conversion (a) and apparent activation energy (b) of NSP catalysts.

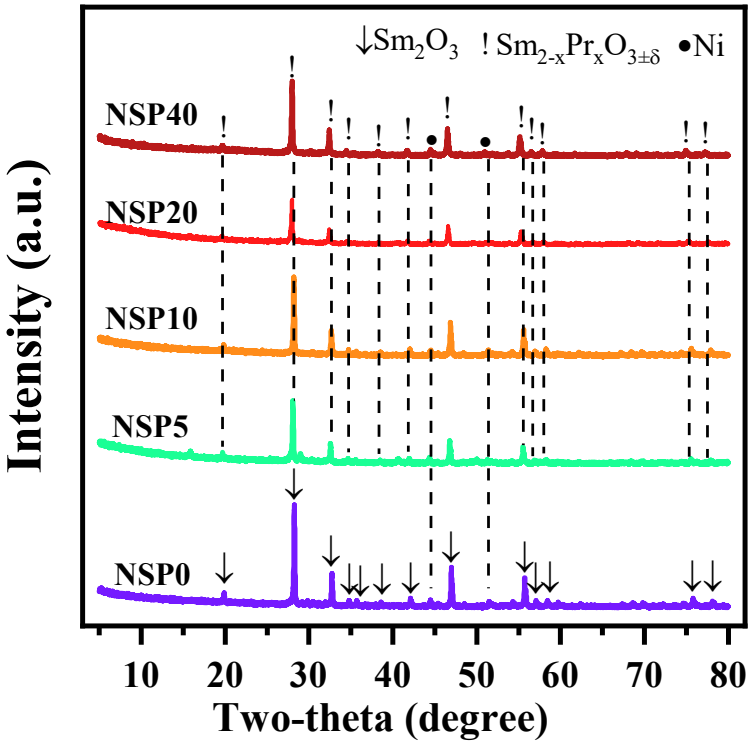

Fig. S2. XRD patterns of the spent catalysts.

Table S1 Ni^0 and supports particle sizes of NSP catalysts and crystal structure data.

catalysts	Crystallite size of Ni^0 estimated by XRD (nm)		Lattice parameters (Å)	d-spacing (Å)	Lattice strain (%)
	Reduce	Spent	a/b/c		
NSP0	57.9	70.8	10.9313	3.1697	0.287
NSP5	55.3	74.5	10.9309	3.1685	0.302
NSP10	53.9	54.8	10.9280	3.1652	0.332
NSP20	49.2	67.4	10.9251	3.1564	0.306
NSP40	45.4	45.7	10.9139	3.1510	0.324

Table S2 Hydrogen consumption and Ni^0 reducibility of NSP catalysts.

Catalysts	Hydrogen consumption (mmol/g)			Ni^0
	Peak1	Peak2	Peak3	Reducibility (%)
NSP0	0.073	0.29	-	17.8
NSP5	0.089	0.31	0.074	19.6
NSP10	0.095	0.38	0.12	23.7
NSP20	0.059	0.42	0.077	23.8
NSP40	0.059	0.54	0.070	29.5

Table S3 The surface compositions of NSP catalysts.

Catalysts	$Ni^0/(Ni^0+Ni^{2+})$		$O_{II}/(O_I+O_{II}+O_{III})$		$Sm^{2+}/(Sm^{2+}+Sm^{3+})$		$Pr^{3+}/(Pr^{3+}+Pr^{4+})$	
	Reduced	Spent	Reduced	Spent	Reduced	Spent	Reduced	Spent
NSP0	27.3%	22.4%	65.3%	60.4%	25.2%	32.0%	-	-
NSP10	30.4%	28.8%	74.5%	73.1%	33.4%	28.7%	36.5%	39.3%
NSP40	~~31.6~~25.1%	20.6%	58.3%	56.2%	30.7%	32.4%	40.8%	33.6%

Table S4 Ni^0 dispersion, Ea and TOF of NSP catalysts.

Catalysts	Ni^0 dispersion [a] (%)	TOF-H_2 [b] (10^{-2} s^{-1})	Ea (KJ/mol)
NSP0	3.6	2.83	62.8
NSP10	24.8	4.99	35.9
NSP40	13.7	3.49	43.8

[a] Obtained from H_2-TPD by assuming H_{ad}/Ni^0_{surf}=1.

[b] Calculated by Equation 5.

Table S5 Comparison of hydrogen production from reforming.

Catalyst	T (°C)	O_2/C	Time (h)	H_2 yield (%)	Ref
$Ni/Ce_{1-x}Y_xO_{2-\delta}$	700	0.28	10	95	[1]
$Ni@SiO_2$-T	750	no statistics	10	58	[2]
$Pt-Al_2O_3$	771	no statistics	2	15	[3]
Co-Ce-O	600	no statistics	10	94	[4]
Co-Ba-Al	650	0.28	10	93	[5]
$Ni/Sm_{2-x}Pr_xO_{3\pm\delta}$	750	0.28	10	98	This work

Reference

1. Su Y, Shu C, Ding C, Chen Q, Xu Y, Sheng J, et al. Solid solution of $Ce_{1-x}Y_xO_{2-\delta}$ supported nickel-based catalysts for auto-thermal reforming of acetic acid with high resistance to coking. 2024:101589.

2. Pu J, Nishikado K, Wang N, Nguyen TT, Maki T, Qian EWJACBE. Core-shell nickel catalysts for the steam reforming of acetic acid. 2018; 224:69-79.

3. Taherian Z, Gharahshiran VS, Khataee A, Orooji YJJoI, Chemistry E. Anti-coking freeze-dried NiMgAl catalysts for dry and steam reforming of methane. 2021; 103:187-194.

4. Hu X, Ding C, Wang Q, Chen H, Jia X, Huang LJICC. Preparation of Co-Ce-O catalysts and its application in auto-thermal reforming of acetic acid. 2022; 141:109537.

5. Xu Y, Song Y, Chen H, Liao F, Huang J, Huang LJJoS-GS, et al. Influence of Ba on Co-Al-Ba composite oxide catalysts in auto-thermal reforming of acetic acid for hydrogen production. 2023; 105(1):202-211.